Date 22 March 2021
Contact Dr. A. Sciacchitano
Telephone +31 (0)15 2788692
Email a.sciacchitano@tudelft.nl

Delft University of Technology

Faculty of Aerospace Engineering
Kluyverweg 1
2629 HS Delft, The Netherlands

TECHNICAL REPORT

Airflow measurements in the Thialf ice rink

Authors:

Dr. Andrea Sciacchitano, Assistant Professor, TU Delft, Faculty of Aerospace Engineering

Prof. Dr. Philo Bluyssen, Chair Indoor Environment, TU Delft, Faculty of Architecture and the Built Environment

Alexander Spoelstra, PhD Student, TU Delft, Faculty of Aerospace Engineering

Laura Jou Ferrer, MSc Student, TU Delft, Faculty of Aerospace Engineering

Abstract

The airflow velocity in the ice rink of Thialf, Heerenveen (the Netherlands), was measured on the 28th of February 2021 by means of large-scale stereoscopic Particle Image Velocimetry (PIV) so as to assess whether the floor grills of the ventilation system induce any tailwind or headwind that could affect the skaters' performances during competitions. The specific questions addressed were:

a) Does the ventilation induce any airflow on the ice rink?
b) Does the airflow velocity change depending of the configuration of the ventilation system?

The measurements were carried out at one location of the skating ring, in absence of audience on the stands and of athletes skating on the track. Different combinations of operations of the ground and ceiling ventilation systems (both on; one on and one off; both off) were analysed, to assess whether changes in the operation of the ventilation system would result in changes in the airflow velocity on the ice rink. A statistical analysis was conducted on the airflow velocity from different measurements to determine the ensemble-averaged airflow velocity at each condition of the ventilation system. The results showed that an airflow velocity between 0.10 m/s and 0.15 m/s in the direction of motion of the skater is produced whenever at least one of the ventilation systems is on. The variations between the different configuration were within the measurement uncertainty. Hence, it is concluded that differences in the airflow velocity on the ice rink between the different configurations are negligible. More detailed studies are required to be able to conclude whether the change of the direction of the grilles in the floor could have affected the direction.

Contents

1 Introduction

Airflow velocity measurements on the ice rink of Thialf were requested to TU Delft to evaluate whether the building's ventilation system induces an airflow that could potentially affect the skaters' performances. In particular, two ventilation systems are present, namely the ceiling ventilation system (composed by outer and inner air socks) and the ground ventilation grills. The nozzles of the outer ventilation system on the ceiling are oriented downwards and slightly in the direction of motion of the skaters. The orientation of the ground grills was modified in November 2020: before the change, the ground air supply was directed vertically and slightly outwards, towards the stands, which create a vertical air-screen between the ice rink and public area; after the change, the ground air supply is directed vertically and slightly in the direction of motion of the skaters. The orientation of the ceiling nozzles and this latter change of the ground grills raised the question of whether the airflow is now inducing a tailwind that could give an advantage to the skaters. Based on the above, the specific questions to be answered in this investigation were:

a) Does the ventilation system induce any airflow on the ice rink?
b) Does the airflow velocity change depending of the configuration of the ventilation system?

To answer these questions, airflow measurements were conducted with different combinations of the ventilation systems on and off (both on; one on and one off; both off). Additionally, changes in the inlet air temperature of the inner ceiling ventilation system were analysed to assess whether those changes, which occurred in two races with and without audience, could affect differently the skaters' performances.

The present report is structured as follows. Section 2 discusses the working principle of the measurement technique employed, the equipment used and its integration in the Thialf ice rink, the selected measurement conditions and the approach for data processing. Section 3 presents the results in terms of measured velocity fields. In particular, sample velocity fields acquired at the different ventilation conditions are shown in Figure 11, and the ensemble-average airflow velocities are summarised in Table 2. Finally, the main conclusions and recommendation for further investigations are summarised in section 4.

2 Experimental setup

2.1 Stereoscopic Particle Image Velocimetry

Flow velocity measurements have been performed by large-scale stereoscopic Particle Image Velocimetry (PIV). The working principle of PIV is based on the measurement of the displacement during a short time interval of small tracer particles travelling within the flow as they are transported at the same velocity as the air stream. A pulsed laser illuminates the particles in a planar measurement domain multiple times at small time separations; the light scattered by the particles at each illumination is recorded by two digital cameras placed at an angle with respect to each other, as schematically illustrated in Figure 1. The measurement of the particle images displacement within the known time interval leads to the computation of the three components of the instantaneous velocity vector within the illuminated plane. More detailed information on PIV is available in standard textbooks such as those by Adrian and Westerweel (2011) and Raffel et al. (2018).

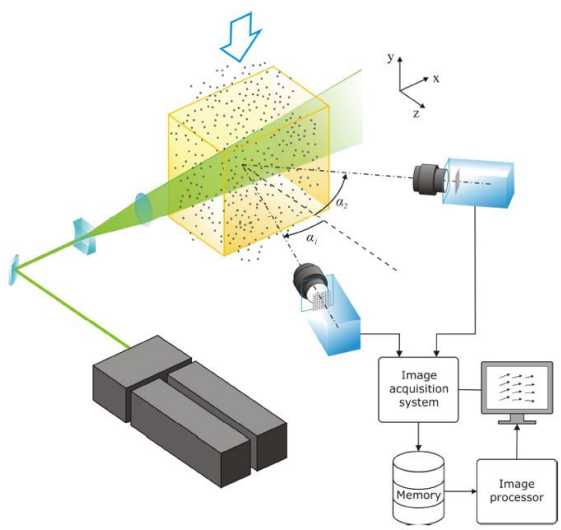

Figure 1. Schematic representation of a typical stereoscopic PIV setup.

2.2 Flow seeding

In the present experiment, the flow was seeded with sub-millimetre neutrally-buoyant Helium-Filled Soap Bubbles (HFSB; Scarano et al., 2015; Faleiros et al., 2018). A seeding rake (hereafter referred to as seeder) developed in-house by TU Delft Aerospace Engineering was employed, composed of 12 wings containing 17 bubble generators each, for a total of 204 generators. The pitch between bubble generators is 5 cm both across and along the wings. Each bubble generator delivers approximately 2×10^6 tracers per second, distributed over an area of 55×80 cm^2 (width × height). The flow rates of the working fluids, namely air, helium and bubble fluid solution, were controlled via a LaVision Fluid Supply Unit (FSU). Pictures of the HFSB seeding rake and the LaVision Fluid Supply Unit are shown in Figure 2.

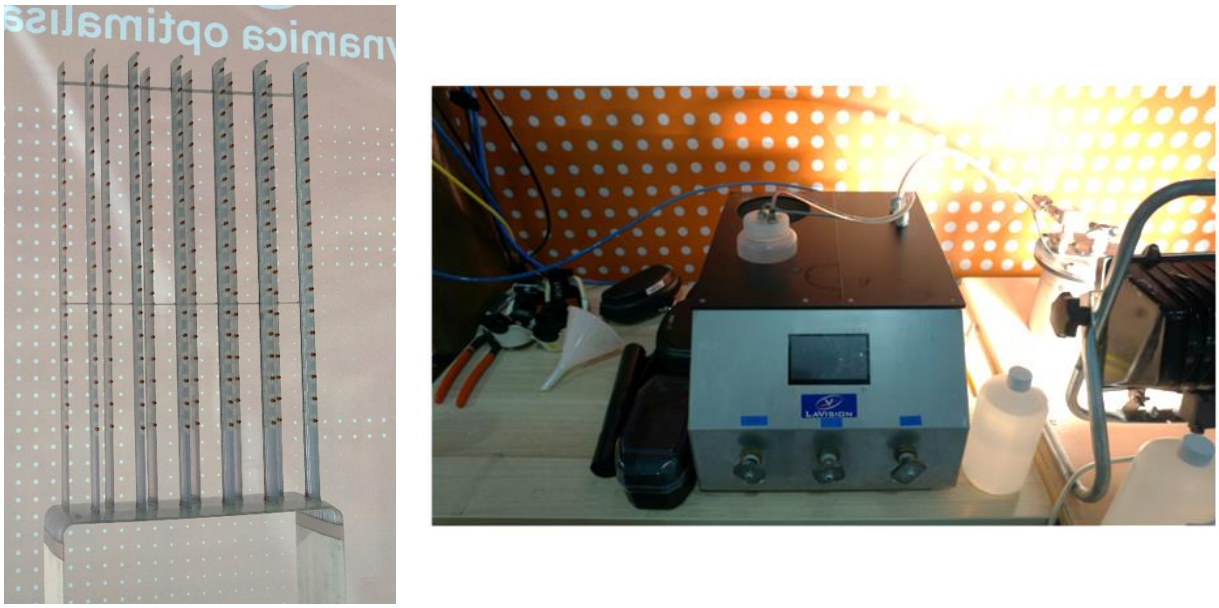

Figure 2. Pictures of the HFSB seeding rake (left) and LaVision Fluid Supply Unit (right).

2.3 Illumination system

The illumination was provided by a Quantronix Darwin Duo Nd:YLF laser 527-80 M laser (dual-cavity, wavelength of 527 nm, 25 mJ pulse energy @ 1 kHz). The laser beam, having a circular cross section of 2 mm diameter at the laser exit, was shaped into a laser sheet of approximately 2 m height and 5 cm thickness by means of a combination of spherical and cylindrical lenses.

Figure 3. Picture of the Quantronix Darwin-Duo laser employed in the measurements.

2.4 Imaging system

Images were recorded by two LaVision HighSpeedStar 6 cameras (CMOS sensor, 12 bit, 1,024 × 1,024 pixels at 5.4 kHz, 20 μm pixel pitch, see Figure 4) in stereoscopic configuration. The sensor size was cropped to 1,024 × 752 (width × height) to limit the imaged area to the region illuminated by the laser light. The cameras mounted Nikkor objectives of 50 mm focal length, set at numerical aperture of 5.6 and 2 for cameras 1 and 2, respectively.

Figure 4. Picture of the LaVision HighSpeedStar 6 cameras employed in the measurements.

2.5 Measurement conditions

The measurements were conducted in the ice rink of Thialf in the morning of Sunday the 28th of February, from 9:00 am until 12:00 pm. All measurements were performed at one location, indicated in Figure 5, in absence of audience on the stands and of any athletes skating in the ice rink.

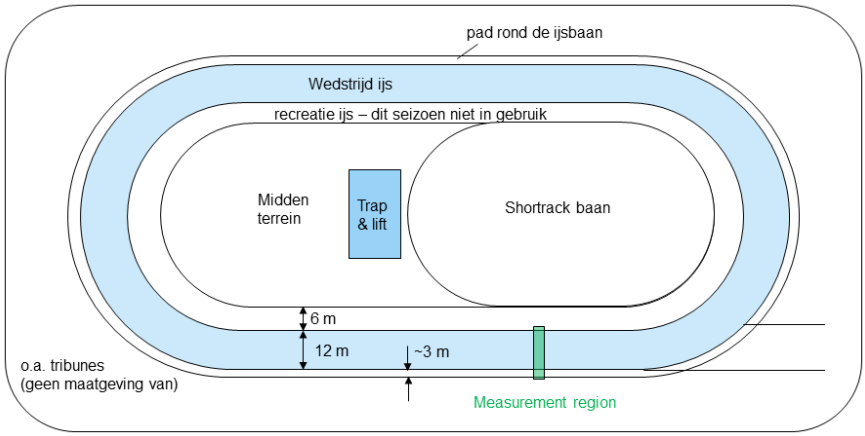

Figure 5. Map of the Thialf ice rink with the measurement region indicated in green.

The ventilation system of Thialf, supplied by the company Warmtebouw, is composed of two separate systems, namely the ceiling air socks and the ground ventilation grills (Figure 6). Measurements have been conducted in five different configurations to assess the relative influence of the two ventilations systems on the airflow on the ice rink:

a) Both systems on, with the inlet air temperature of the inner ceiling ventilation system set to 27 °C;
b) Only ceiling ventilation system on, with the inlet air temperature of the inner ceiling ventilation system set to 27 °C;
c) Only ground ventilation system on;
d) Both systems off;
e) Both systems on, with the inlet air temperature of the inner ceiling ventilation system set to 16 °C.

Figure 6. Picture of the ceiling air socks and ground ventilation grills in the Thialf ice rink.

It should be noticed that the ventilation systems operate always at the same volume flow rate, which is not regulated/influenced by the building management system. The air temperature of the inner ceiling ventilation system can be regulated to maintain a constant room temperature, and was varied during the

measurements. During races, the inlet air temperature of the inner ceiling ventilation system is set such that the room temperature in the ice rink is constant and equal to about 14°C. The two values of inlet air temperature considered in the measurements, namely 16°C and 27°C, correspond to typical values set during competitions with and without (due to covid restrictions) audience on the stands, respectively. These measurements were performed to assess whether changes in the inlet temperature affect the airflow velocity on the rink. It should be remarked that the measurements were conducted without audience on the stands. The ventilation configuration with 16°C inlet temperature is never achieved in actual races without audience; however, it was tested because it likely provides an upper limit to the airflow velocity achievable on the ice rink.

The air temperature of the outer ceiling ventilation system and of the ground ventilation system can be regulated within a small range (between 20 and 24°C) depending on the difference between measured and set-point return air temperature; such temperature was not changed during the measurements.

2.6 Integration of the large-scale stereoscopic PIV system into the Thialf ice rink

A metal structure was built on the sides of the ice rink to mount the digital cameras, as illustrated in Figure 7. The cameras were at a distance of about 6 m from the measurement plane, and formed a stereoscopic angle of about 90 degrees, which is the optimal one for the measurement of the out-of-pane velocity component (Prasad, 2000). A schematic of the experimental setup is shown in Figure 8.

The stereoscopic calibration was performed using the pinhole model, after which a self-calibration based on the particle images was carried out (Wieneke, 2005). After stereoscopic reconstruction, the imaged field of view had a size of 4483 × 2608 mm (width × height, as illustrated in Figure 9), resulting in a digital image resolution of 3.1 mm/pixel (optical magnification factor: 0.006).

The laser light was provided from the inner side of the ice rink. The seeding rake was placed at a distance of at least 4.5 m from the measurement plane, with the normal to the seeder in the same direction as the laser sheet so as to minimise the influence of the bubbles injection onto the flow velocity measurements. The exact location and orientation of the seeding rake were varied slightly among the measurement conditions to ensure a uniform distribution of the flow tracers in the entire measurement domain (see Figure 10). Those changes had no effect on the measured airflow velocity due to the large distance between the seeder and the measurement region.

For each measurement conditions, at least 3 sets of 1,000 image recordings each were acquired in continuous mode at the acquisition frequency of 200 Hz (time between successive images: Δt = 5 ms). Image acquisition and processing were carried out with the Davis 8.4 software from LaVision GmbH. The waiting time between one image acquisition and the successive one of the same measurement condition was about 2 minutes. Instead, the waiting time between two image acquisitions of different measurement conditions was 15 minutes so as to eliminate any transient effects associated with turning on or off the ventilation systems.

The achieved seeding density varied from run to run, but was in the order of 0.05 particles per pixels (ppp). Regions of low seeding density (below 0.01 ppp) were blanked out and not considered for further analysis.

Figure 7. Metal structure holding the high-speed digital cameras. During the day of the measurements for the Thialf ventilation system, no curtains nor banners were applied to the metal structures so as not to affect the air flow.

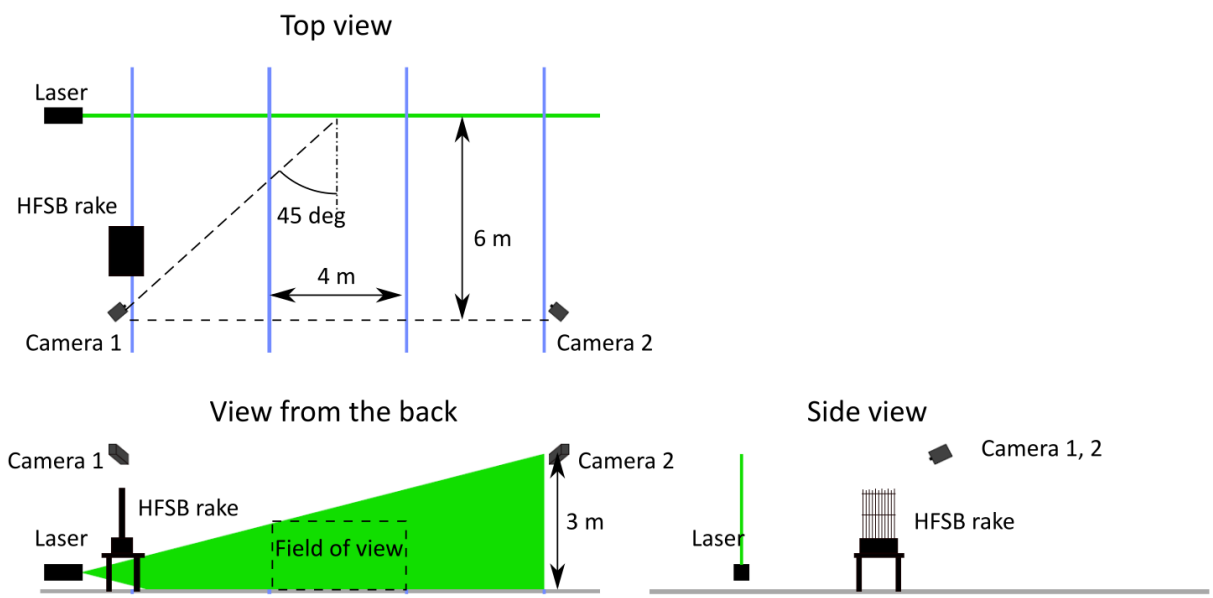

Figure 8. Schematics of the experimental setup.

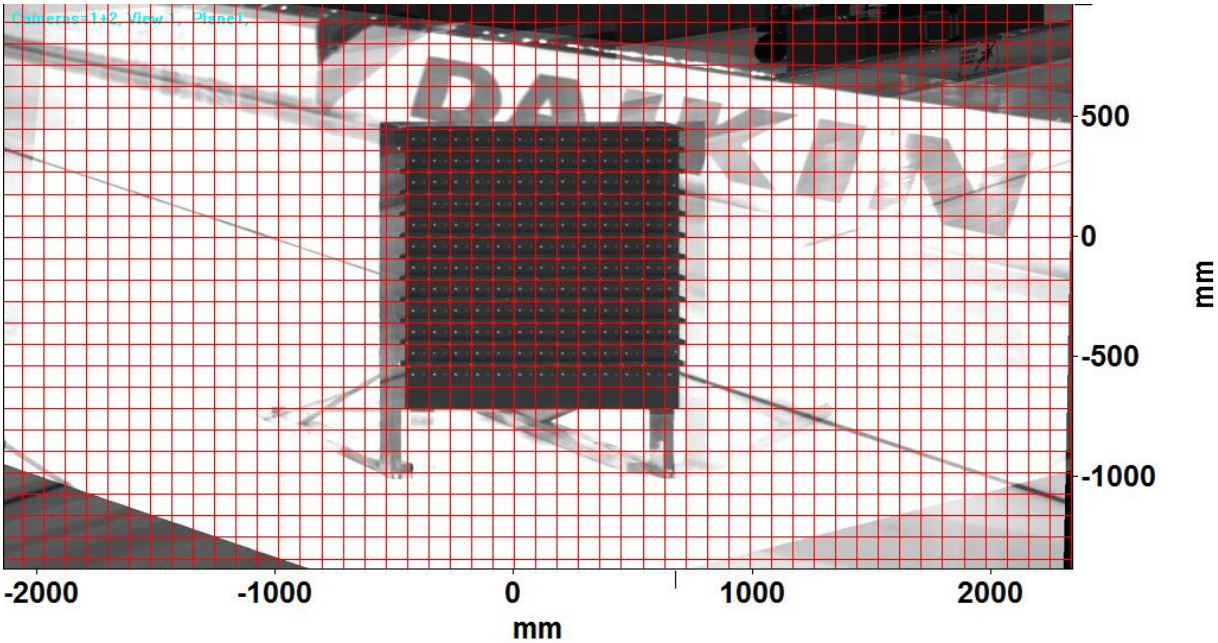

Figure 9. Dewarped image (in world coordinates) of the calibration plate.

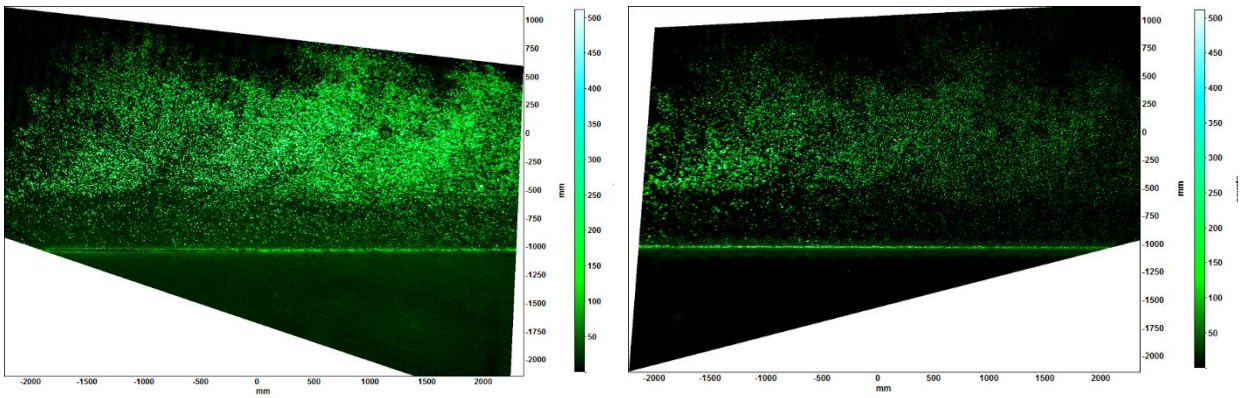

Figure 10. Sample images of camera 1 (left) and camera 2 (right) after dewarping from raw to world coordinates.

2.7 Data processing and measurement uncertainty

Image pre-processing was carried out by subtraction of the pixel-wise minimum intensity in time over each set of images, so as to eliminate unwanted laser light reflections (Adrian and Westerweel, 2011). The pre-processed images were then analysed in the LaVision Davis 8.4 software via an iterative cross-correlation-based algorithm with image deformation (Scarano, 2001). The interrogation window size was decreased from 128 × 128 pixels to 64 × 64 pixels; for both window sizes, 2 iterations, Gaussian weighting and 75% overlap factors were applied. The resulting pitch between adjacent vectors was equal to 50 mm. A 6-point bi-cubic spline image interpolation algorithm was used for the final passes to increase the sub-pixel accuracy and reduce peak-locking errors. The images were processed with a skip of 10 (effective time separation between images analysed: 50 ms) to increase the average particle image displacement, thus reducing the relative measurement uncertainty.

For each run, the time-average velocity field was computed as:

$$\overline{V} = \frac{1}{M}\sum_{i=1}^{M} V_i \tag{1}$$

where V_i is the instantaneous velocity field, and M the number of velocity fields of each run.

Then, for each run, the time-average velocity was averaged spatially in a square box of L = 1.2 m edge (from the ground to 1.2 m above the ground, and placed in the middle lane), obtaining the spatially-averaged velocity $\hat{V}$. Notice that 1.2 m above the ground is the typical height reached by the skaters during their motion. Finally, the spatially-averaged velocity was averaged among different runs of the same measurement condition to determine the ensemble-average velocity for that condition:

$$\langle V \rangle = \frac{1}{N}\sum_{i=1}^{N} \hat{V}_i \tag{2}$$

where N is the number of runs at a given measurement condition.

The measurement uncertainty is expressed at 95% confidence level as:

$$U = \frac{t_{95} \cdot s}{\sqrt{N}} \tag{3}$$

where t_{95} is the coverage factor for the t-distribution with $\nu = N$-1 degrees of freedom (see Coleman and Steele, 2018; t_{95} = 4.303 for N = 3; t_{95} = 2.365 for N = 8) and s the sample standard deviation of the $\hat{V}$ of a given measurement condition.

2.8 Test matrix

The test matrix of the measurements is reported in Table 1. It is remarked that more measurements (namely 8) were conducted with only the ground ventilation system on (contrary to 3 measurements for each of the other ventilation conditions). This choice was made due to the particular interest in determining whether the ground ventilation system produced an airflow on the ice rink, which had been speculated after the recent change of the grills orientations.

Table 1. Test matrix of the measurements.

Run #	Time	Meas. condition	f_{acq} [Hz]	# images	f# cam 1	f# cam 2	Notes[1]
Run001	09:07	Both ventilations	200	1000	2	5.6	Ceiling inner ventilation temp. 27°C
Run002	09:10	Both ventilations	200	1000	2	5.6	Ceiling inner ventilation temp. 27°C
Run003	09:12	Both ventilations	200	1000	2	5.6	Ceiling inner ventilation temp. 27°C
Run004	09:26	Ceiling ventilation only	200	1000	2	5.6	Ceiling inner ventilation temp. 27°C
Run005	09:28	Ceiling ventilation only	200	1000	2	5.6	Ceiling inner ventilation temp. 27°C
Run006	09:30	Ceiling ventilation only	200	1000	2	5.6	Ceiling inner ventilation temp. 27°C
Run007	09:46	Ground ventilation only	200	1000	2	5.6	
Run008	09:51	Ground ventilation only	200	1000	2	5.6	
Run009	10:01	Ground ventilation only	200	1000	2	5.6	Seeder moved away from the laser sheet
Run010	10:07	Ground ventilation only	200	1000	2	5.6	Seeder moved closer from the laser sheet
Run011	10:13	Ground ventilation only	200	1000	2	5.6	Seeder turned against the skating direction (angle between normal to the seeder and skating direction ~110 deg)
Run012	10:18	Ground ventilation only	200	1000	2	5.6	As Run011
Run013	10:35	No ventilation	200	1000	2	5.6	Seeder turned in the skating direction (angle between normal to the seeder and skating direction ~70 deg) Person passed through the laser sheet before the measurement to increase the

[1] Unless stated otherwise, the seeder is positioned in such a way that its normal is perpendicular to the skating direction.

							bubbles' concentration in the measurement domain
Run014	10:40	No ventilation	200	1000	2	5.6	As Run013
Run015	10:45	No ventilation	200	1000	2	5.6	As Run013
Run016	11:08	Both ventilations	200	1000	2	5.6	Normal to the seeder perpendicular to the skating direction; seeder moved to middle lane. Ceiling inner ventilation temp. 16°C
Run017	11:10	Both ventilations	200	1000	2	5.6	As Run016
Run018	11:14	Both ventilations	200	1000	2	5.6	As Run016
Run019	11:30	Ground ventilation only	200	1000	2	5.6	Seeder moved to the inner edge of the middle lane; normal to the seeder perpendicular to the skating direction
Run020	11:32	Ground ventilation only	200	1000	2	5.6	As Run019

3 Results

3.1 Airflow velocity

Sample results of the different measurement conditions are shown in Figure 11 in terms of contours of the time-average out-of-plane velocity component Vz and in-plane velocity vectors[2]. All time-average velocity fields are reported in Appendix A for completeness. Notice that negative values of Vz correspond to an airflow in the direction of motion of the skater (tailwind), whereas positive values of Vz indicate an airflow opposite to the direction of motion of the skater (headwind). The square area where the statistical analysis is conducted, as well as the reference in-plane vector of 0.2 m/s, are also illustrated in Figure 11-top.

When both ventilation systems are on (Figure 11-top), the airflow is in the direction of motion of the skater with velocities up to –0.25 m/s. Similar flow fields are retrieved also when only the ceiling ventilation is on (Figure 11, second row), with slightly lower velocities. When only the ground ventilation system is on, the flow field is divided into two regions: a bottom region up to about 400 mm from the ground, where the air slowly flows against the direction of motion of the skater (Vz < 0.05 m/s), and a top region above 400 mm from the ground where the air flows in the direction of motion of the skater (Vz up to –0.20 m/s).

The statistical results in the square of 1.2 m edge shown in Figure 11-top are summarised in Table 2. Variations of the spatially-averaged airflow velocity are measured among different runs of the same measurement condition, which are ascribed to the unsteadiness of the flow and to the limited measurement time (5 seconds) of each run. However, at any given measurement condition, the spatially-averaged velocity does not change sign from run to run, meaning that the airflow has always a preferential direction, that is the direction of motion of the skater.

From the results of Table 2, it is clear that, when both ventilations systems are turned off, the measured airflow velocity is within the measurement uncertainty (Vz = –0.020±0.028 m/s), meaning that the airflow is negligible. In all the other measurement configurations, an airflow velocity exceeding 0.10 m/s in the direction of motion of the skaters is measured. The differences in airflow velocity among different configurations of the ventilation system are within the measurement uncertainty, which is attributed to the unsteadiness of the flow and the limited number of measurements per configuration. Hence, it is concluded that the tested variations of the ventilation system configurations have negligible effect onto the airflow velocity on the ice rink.

Also, it should be remarked that the ensemble average airflow velocities in the different ventilation configurations are below the limit (0.2 m/s) defined by the Dutch Building Decree (http://www.onlinebouwbesluit.nl/) and ASHRAE Standard 55-2017 (American Society of Heating, Refrigerating and Air-Conditioning Engineers) for the occupied zone of an area where people stay. Furthermore, the measured air velocity is well below the limit (0.5 m/s) imposed by the code norm NOCNSF-US1-RU.1 for covered multidisciplinary sports facility (not specifically for ice skating[3]).

[2] The time-average velocity component in the skating direction is hereafter indicated as Vz rather than $\overline{Vz}$.

[3] To the best of the authors' knowledge, no quantitative value for the maximum airflow velocity in an ice rink is provided by the International Skating Union (ISU) to guarantee fair competitions.

Table 2. Ensemble-average airflow velocity (in metres per second) in the skating direction depending on the ventilation system used in the ice rink. Negative values correspond to an airflow in the direction of motion of the skater (tailwind); positive values indicate an airflow against the direction of motion of the skater (headwind).

	Both on (inner T = 27°C)[4]	**Ceiling on (inner T = 27°C)**	**Ground on**	**Both off**	**Both on (inner T = 16°C)[5]**
Run A	-0.097	-0.146	-0.093	-0.007	-0.173
Run B	-0.126	-0.083	-0.091	-0.025	-0.130
Run C	-0.138	-0.098	-0.155	-0.028	-0.139
Run D			-0.197		
Run E			-0.101		
Run F			-0.135		
Run G			-0.177		
Run H			-0.109		
Total	**-0.121±0.052**	**-0.109±0.082**	**-0.132±0.034**	**-0.020±0.028**	**-0.148±0.056**

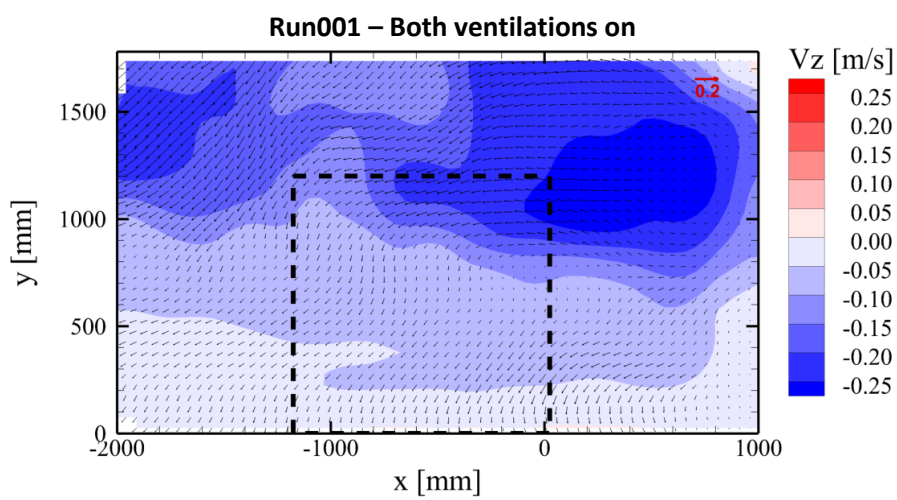

[4] This configuration corresponds to the typical ventilation of a race in absence of audience on the stands.

[5] This configuration is an extreme case that is never achieved in actual races. In fact, in absence of audience on the stands, the inlet ceiling ventilation temperature is kept to around 27°C to keep the room temperature to 14°C. The inlet temperature would be reduced to 16°C only in presence of audience in the stands; however, the current measurements were conducted without audience.

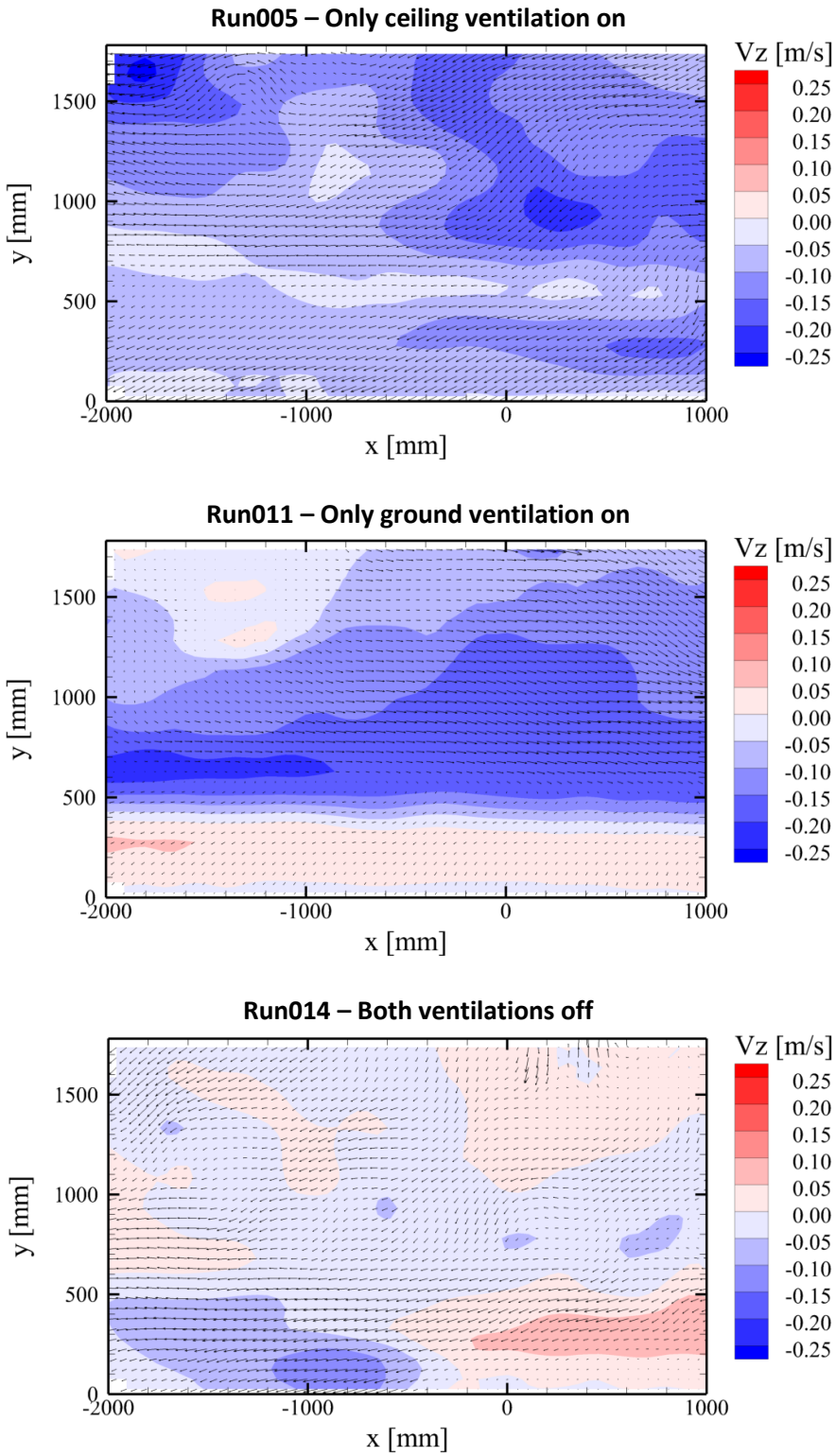

Figure 11. Sample velocity fields measured with both ventilation systems on (top row), only ceiling ventilation system on (second row), only ground ventilation system on (third row) and both ventilation systems off (fourth row). Contours of the time-average velocity component in the direction of the skater's motion, with in-plane velocity vectors: negative values of Vz correspond to an airflow in the direction of motion of the skater (tailwind); positive values of Vz indicate an airflow opposite to the direction of motion of the skater (headwind). The reference in-plane vector of 0.2 m/s is shown in red in the top-right corner of the top figure. Also, the square area where the statistical analysis is conducted is illustrated with a dashed black line in the top figure.

4 Conclusions and recommendations for future investigations

Based on the large-scale stereoscopic Particle Image Velocimetry measurements performed in the Thialf ice rink, the following conclusions can be drawn on the airflow velocity induced by the ventilation system:

a) Does the ventilation induce any airflow on the ice rink?

Yes, the ventilation system induces an airflow in the direction of motion of the skater, having a magnitude of about 0.10 m/s. Such airflow velocity is below the limit (0.5 m/s) defined by the NOC*NSF for a multidisciplinary sports-facility (https://sportvloeren.sport.nl/normen/58-nocnsf-us1-ru1) and ASHRAE Standard 55-2017 (American Society of Heating, Refrigerating and Air-Conditioning Engineers) for the occupied zone of an area where people stay.

b) Does the airflow velocity change depending of the configuration of the ventilation system?

The changes of the airflow velocity with the ventilation system configuration were within the measurement uncertainty. Hence, it is concluded that differences in the airflow velocity on the ice rink between the different configurations are negligible. However, more detailed studies are required to be able to conclude whether the change of the direction of the grilles in the floor could have affected the direction.

It is remarked that the current measurements were performed at one location of the skating ring of Thialf, in absence of audience on the stands and of athletes skating on the track. To complement the present measurements, further studies are advised to investigate:

- Whether changing the orientation of the ventilation grills on the ground affects the induced airflow;
- Whether the airflow velocity is constant along the track, or any variations along the track are present;
- Whether the presence of audience on the stands affects the airflow velocity on the track;
- How the presence of athletes skating on the track or warming up outside of the track affects the airflow induced by the ventilation systems;

Furthermore, it is recommended to benchmark the airflow velocity induced by the ventilation systems in other skating rinks to assess the differences among skating rinks.

5 References

Adrian L, Adrian RJ, Westerweel J. Particle image velocimetry. Cambridge university press; 2011

ASHRAE (2017) ANSI/ASHRAE standard 55-2017, Thermal environmental conditions for human occupancy, Atlanta, USA.

Coleman HW, Steele WG. Experimentation, validation, and uncertainty analysis for engineers. John Wiley & Sons; 2018 May 8.

Faleiros DE, Tuinstra M, Sciacchitano A, Scarano F. Generation and control of helium-filled soap bubbles for PIV. Experiments in Fluids. 2019 Mar;60(3):1-7

Prasad AK. Stereoscopic particle image velocimetry. Experiments in fluids. 2000 Aug;29(2):103-16

Raffel M, Willert CE, Scarano F, Kähler CJ, Wereley ST, Kompenhans J. Particle image velocimetry: a practical guide. Springer; 2018 Apr 3

Scarano F, Ghaemi S, Caridi GC, Bosbach J, Dierksheide U, Sciacchitano A. On the use of helium-filled soap bubbles for large-scale tomographic PIV in wind tunnel experiments. Experiments in Fluids. 2015 Feb;56(2):1-2

Scarano F. Iterative image deformation methods in PIV. Measurement science and technology. 2001 Nov 23;13(1):R1

Timmer N, Veldhuis L. The impact of skinsuit zigzag tape turbulators on speed skating performance. Applied Sciences. 2021 Jan;11(3):988

Wieneke B. Stereo-PIV using self-calibration on particle images. Experiments in fluids. 2005 Aug;39(2):267-80

Appendix A – Velocity fields

The time-averaged velocity fields corresponding to all the measurements are reported hereafter. The regions were no velocity information could be collected because of the lack of tracer particles have been blanked. The reference in-plane vector of 0.2 m/s is indicated in the top-right of each figure.

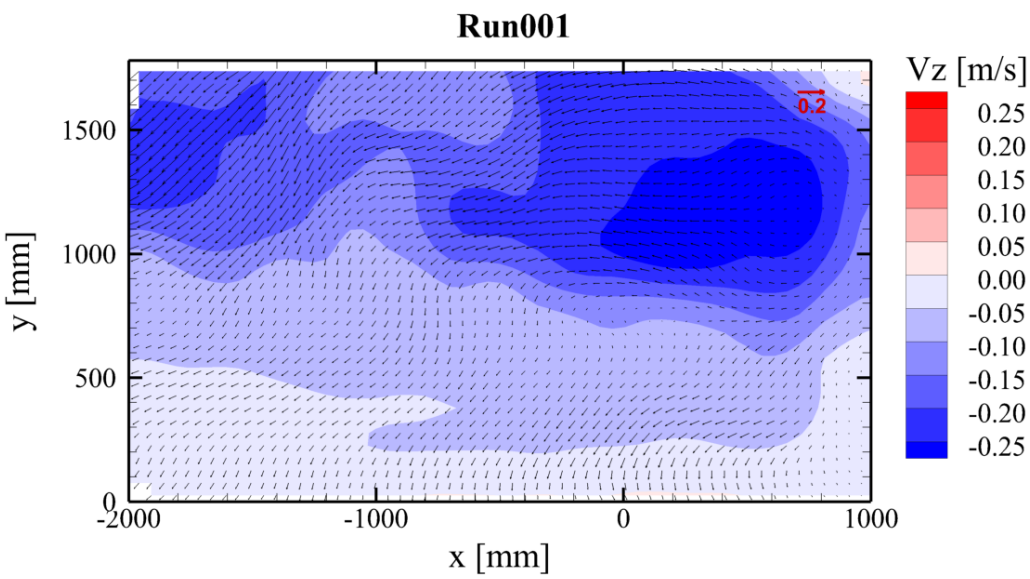

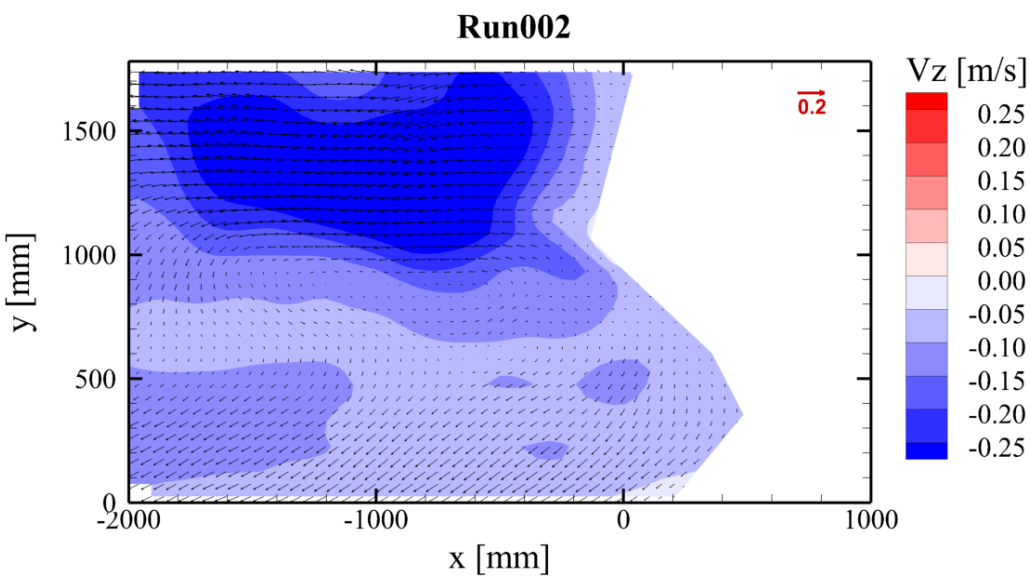

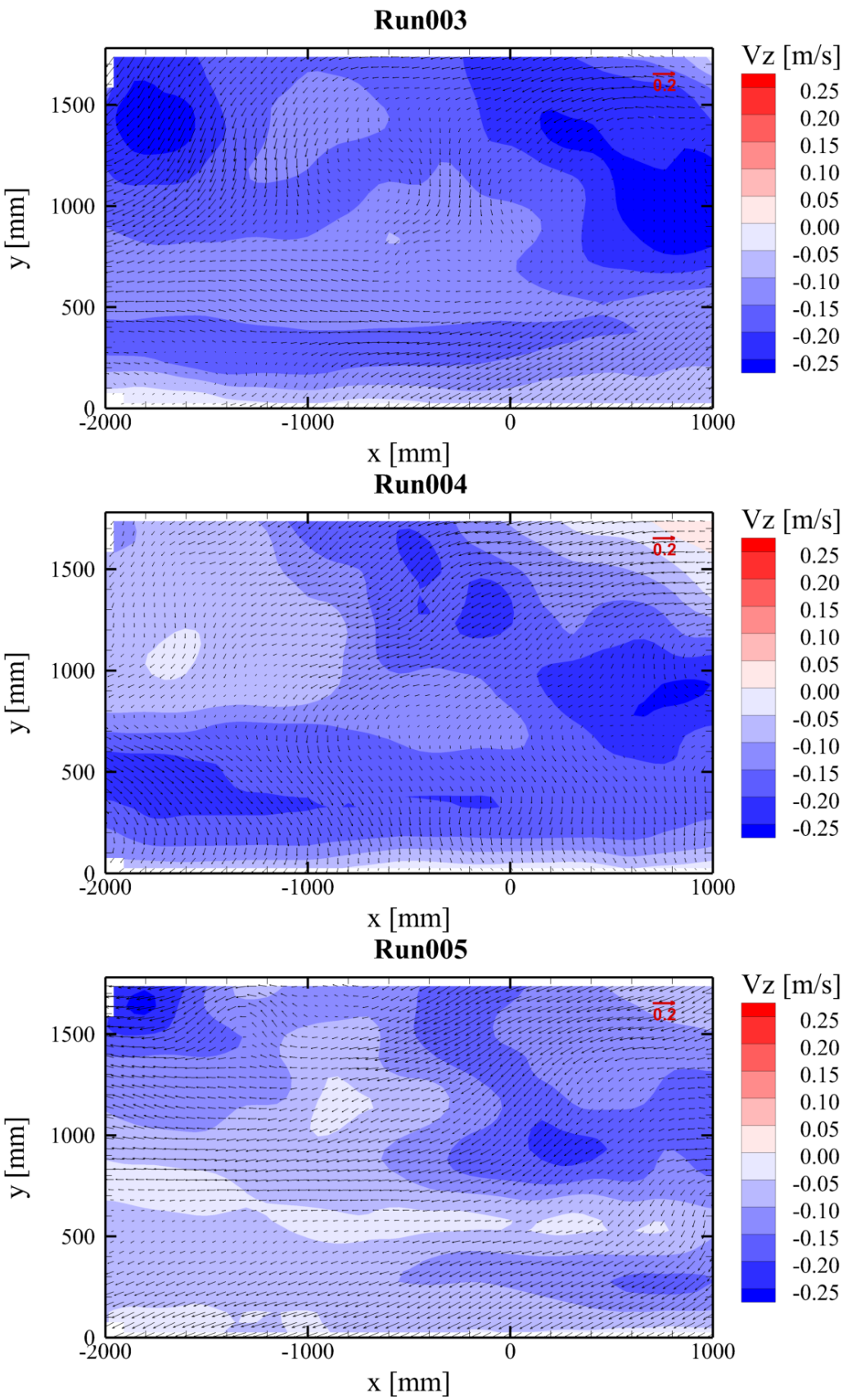
Run003
Run004
Run005
Vz [m/s]
0.25
0.20
0.15
0.10
0.05
0.00
-0.05
-0.10
-0.15
-0.20
-0.25
0.2
y [mm]
x [mm]
0
500
1000
1500
-2000
-1000
0
1000

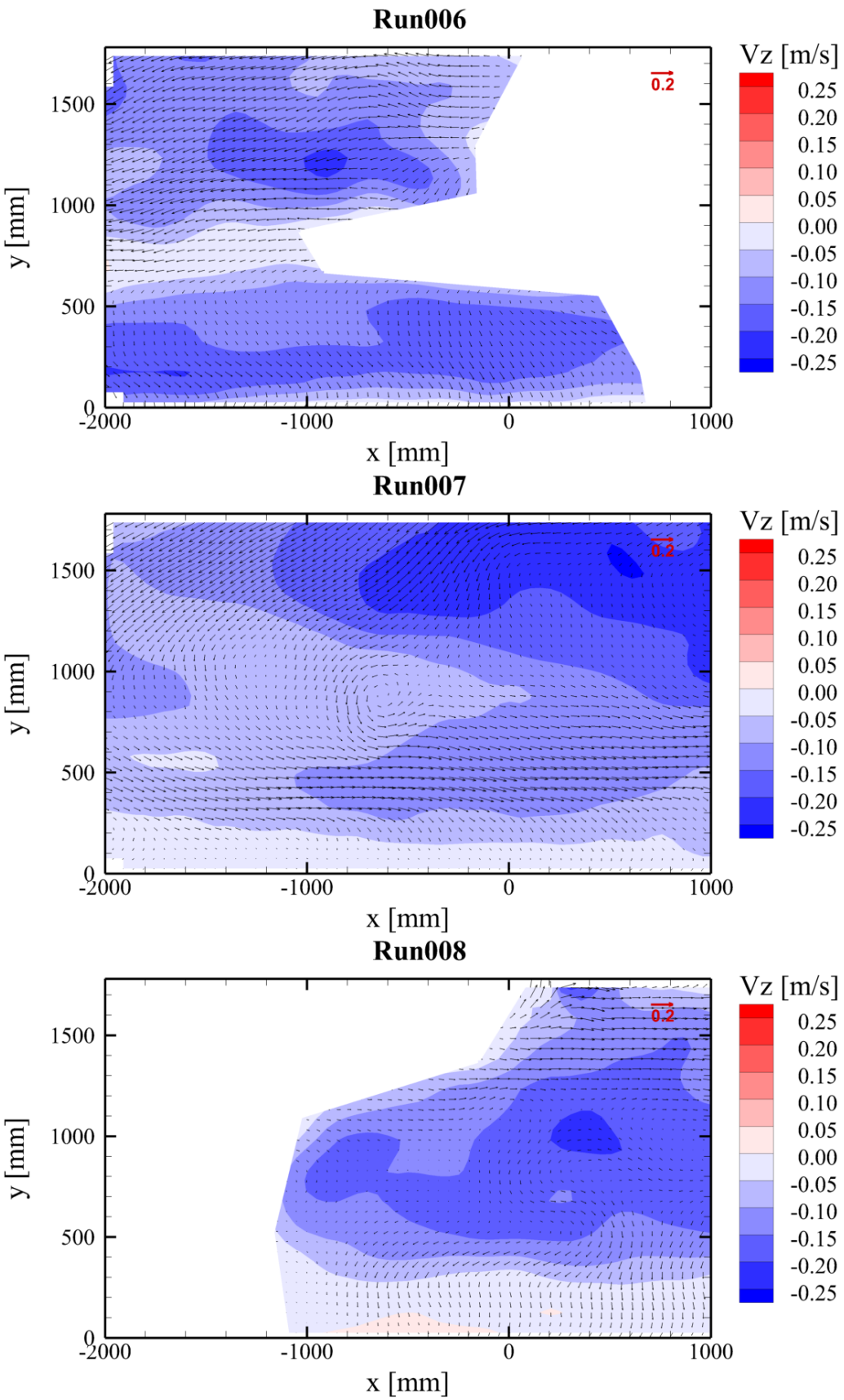
Run006
Run007
Run008
Vz [m/s]
0.25
0.20
0.15
0.10
0.05
0.00
-0.05
-0.10
-0.15
-0.20
-0.25
0.2
y [mm]
x [mm]
0
500
1000
1500
-2000
-1000
0
1000

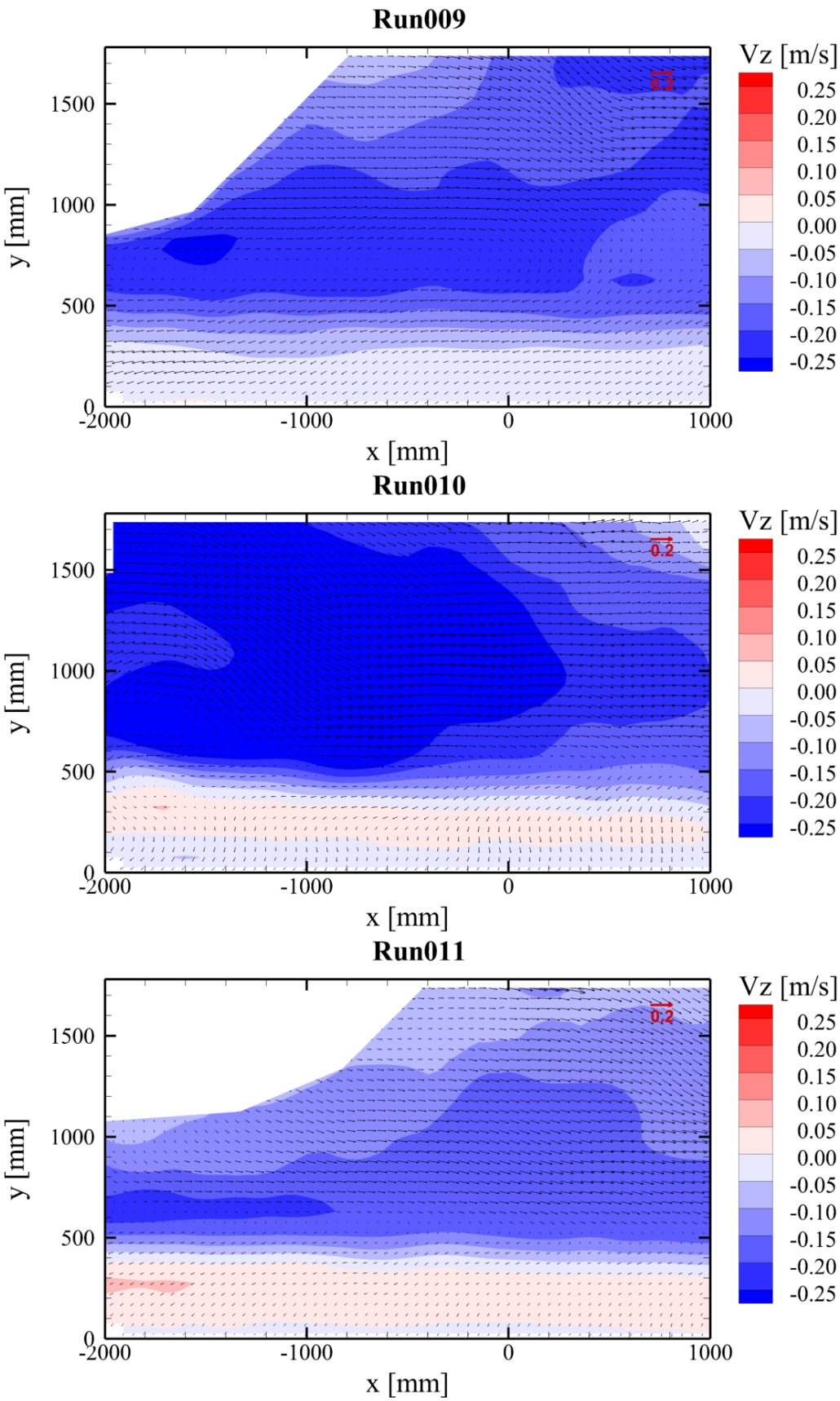
Run009
Run010
Run011
Vz [m/s]
0.25
0.20
0.15
0.10
0.05
0.00
-0.05
-0.10
-0.15
-0.20
-0.25
0.2
y [mm]
x [mm]
0
500
1000
1500
-2000
-1000
0
1000

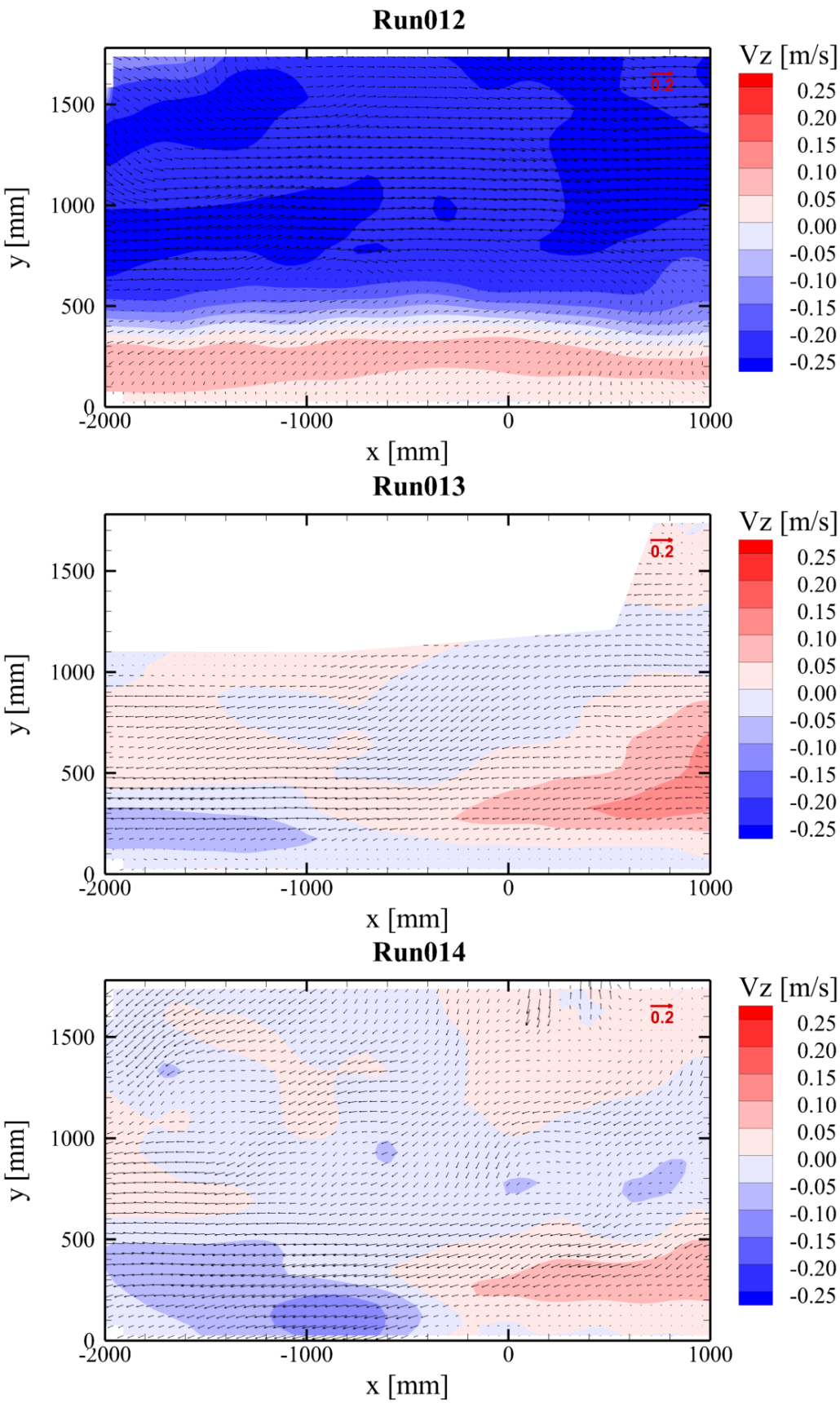
Run012
Run013
Run014
Vz [m/s]
0.25
0.20
0.15
0.10
0.05
0.00
-0.05
-0.10
-0.15
-0.20
-0.25
0.2
y [mm]
x [mm]
0
500
1000
1500
-2000
-1000
0
1000

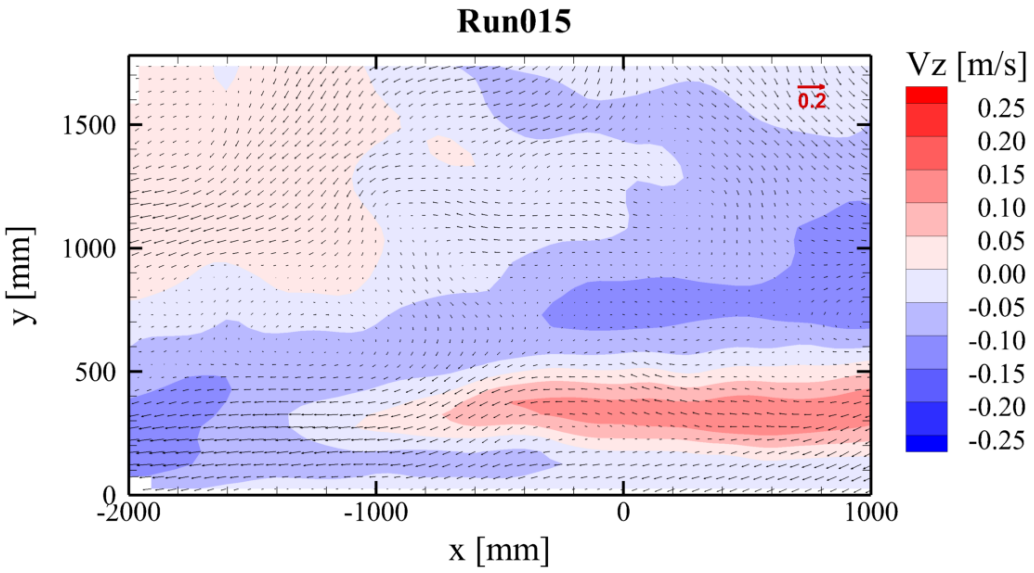
Run015
Vz [m/s]
0.25
0.20
0.15
0.10
0.05
0.00
-0.05
-0.10
-0.15
-0.20
-0.25
0.2
y [mm]
x [mm]
0
500
1000
1500
-2000
-1000
0
1000

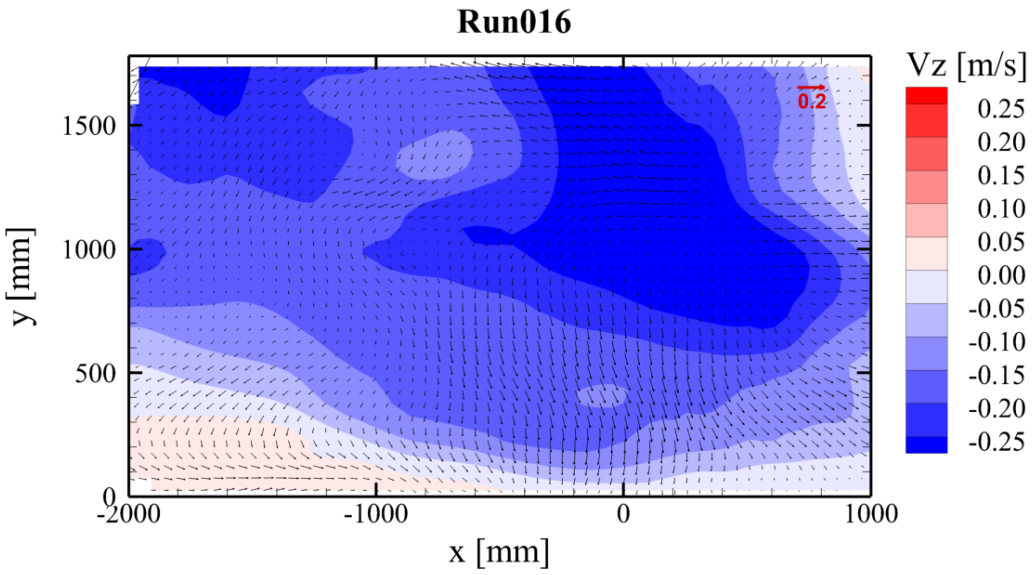
Run016
Vz [m/s]
0.25
0.20
0.15
0.10
0.05
0.00
-0.05
-0.10
-0.15
-0.20
-0.25
0.2
y [mm]
x [mm]
0
500
1000
1500
-2000
-1000
0
1000

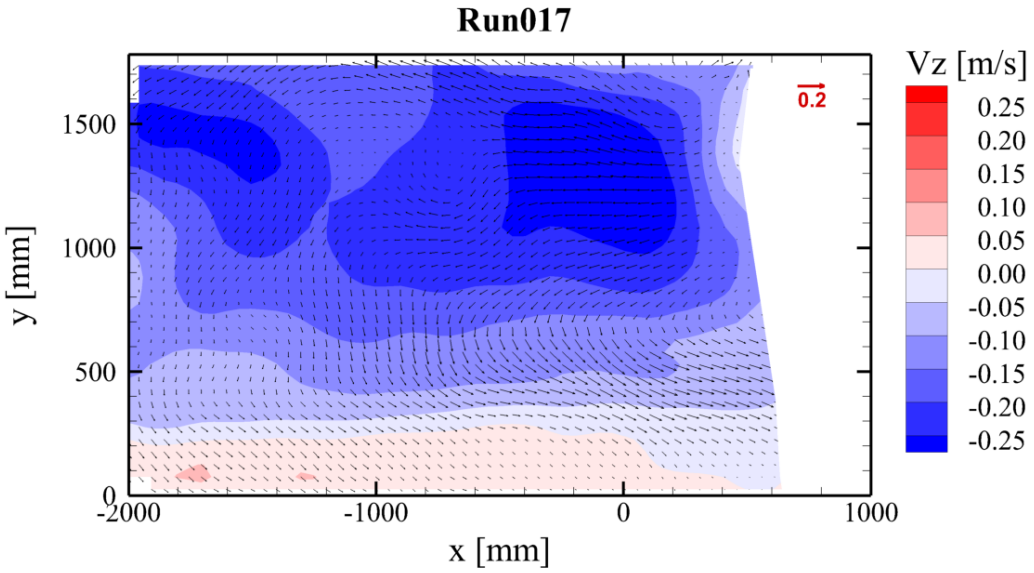
Run017
Vz [m/s]
0.25
0.20
0.15
0.10
0.05
0.00
-0.05
-0.10
-0.15
-0.20
-0.25
0.2
y [mm]
x [mm]
0
500
1000
1500
-2000
-1000
0
1000

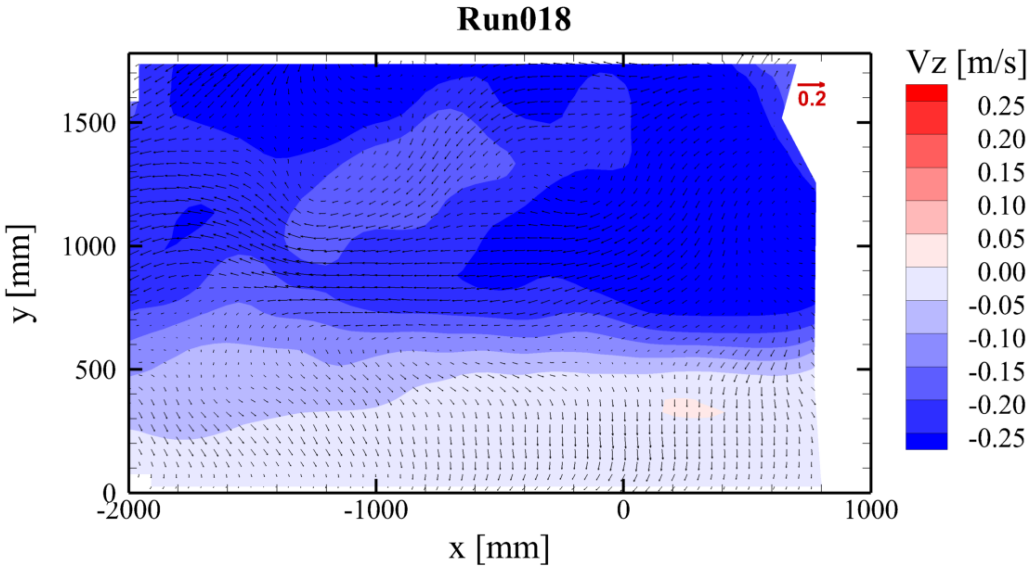
Run018
Vz [m/s]
0.25
0.20
0.15
0.10
0.05
0.00
-0.05
-0.10
-0.15
-0.20
-0.25
0.2
y [mm]
x [mm]
0
500
1000
1500
-2000
-1000
0
1000

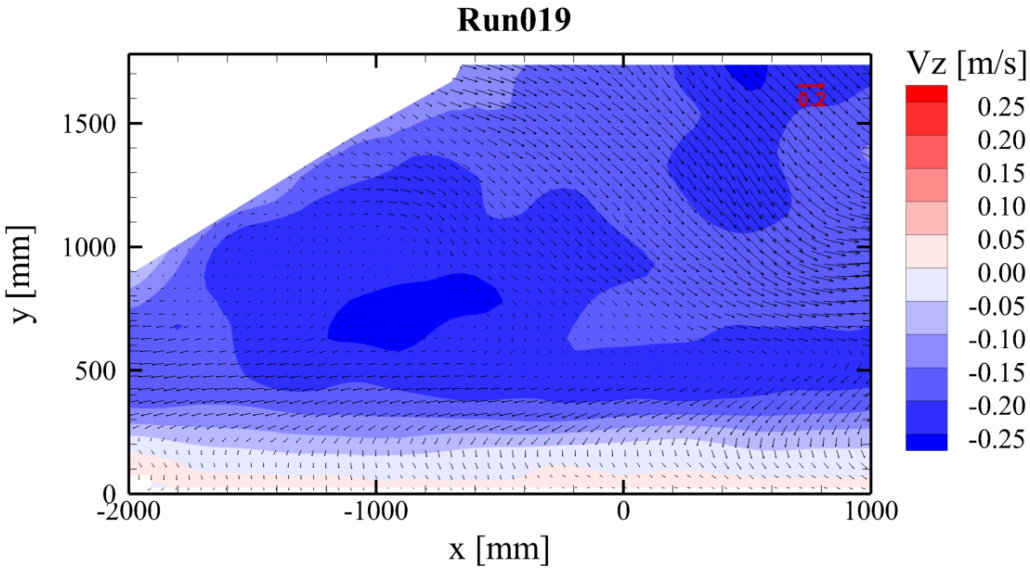
Run019
Vz [m/s]
0.25
0.20
0.15
0.10
0.05
0.00
-0.05
-0.10
-0.15
-0.20
-0.25
0.2
y [mm]
x [mm]
0
500
1000
1500
-2000
-1000
0
1000

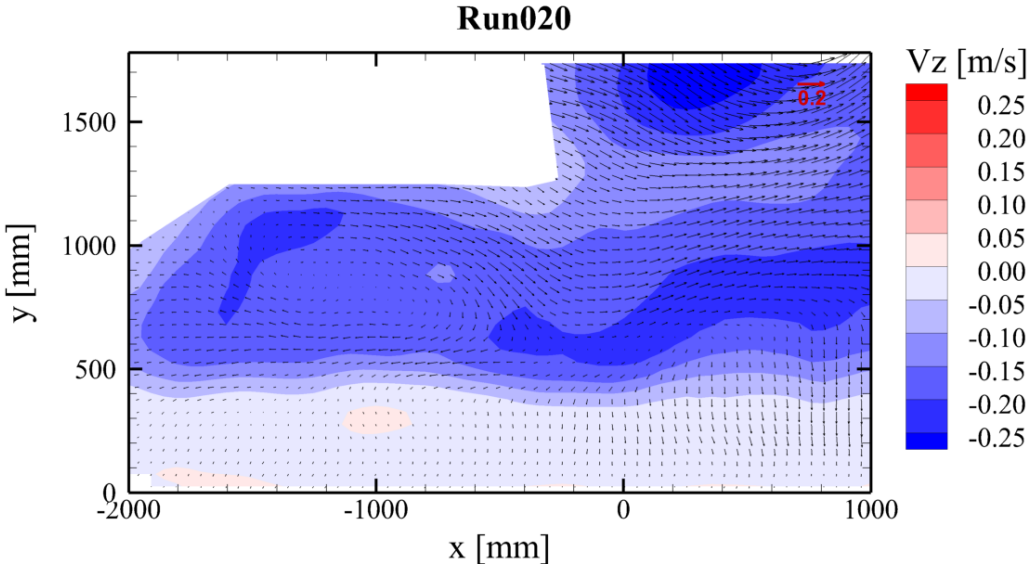
Run020
Vz [m/s]
0.25
0.20
0.15
0.10
0.05
0.00
-0.05
-0.10
-0.15
-0.20
-0.25
0.2
y [mm]
x [mm]
0
500
1000
1500
-2000
-1000
0
1000

Appendix B – Air socks flow rate

The flow rate of the air socks on the ceiling on the date of the measurements is reported below.